2022

Challenges of Constructing Entrainment Map for Arbitrary Circadian Models

Yuxuan (Nelson) Wu
Colby College

Challenges of Constructing Entrainment Map for Arbitrary Circadian Models

An Honors Thesis
Presented to
Professor Stephanie Taylor of the Department of Computer Science
Colby College
In partial fulfillment of the requirements for the
Degree of Bachelor of Arts
By
Yuxuan (Nelson) Wu
Waterville, Maine
May 10th, 2022

Abstract

The entrainment map, developed by Dr.Diekman and Dr.Bose, is claimed to be a 1-dimensional map that produces a better prediction for phase-locking than methods than the phase response curve for circadian models. In his paper [2], he constructs the entrainment map for the two-dimensional circadian model, the Novak-Tyson model, and the other two higher-dimensional circadian models. For this thesis, we concentrate on exploring if it is viable to construct the entrainment map for other circadian models that are not included in his paper: the Becker-Weimann model and the Relogio model. In addition, we discuss the challenges of constructing the entrainment map in general.

Acknowledgements

We thank for Professor Stephanie Taylor for agreeing to be the advisor for this thesis. In addition, we also thank for Professor Stephanie Taylor for her consistent support and mentorship throughout the last two years. This thesis cannot be completed without her help.

Contents

1 Introduction

The physical, psychological, and behavioral changes that follow a 24-hour cycle are commonly defined as the circadian rhythm. This natural process which predominantly responds to light and dark affects most creatures, including humans. One of the most common examples of a light-related circadian rhythm is sleeping at night and being awake during the day [1]. For instance, consider if one individual usually goes to sleep at around 10 pm and wakes up around 6:30 am for a usual day. On a Wednesday, it is invited to a party, and it stays awake until 4 am. It sleeps and wakes up until noon. Then, unfortunately, it takes several days of a chaotic sleep-wake pattern for it to regain its regular resting schedule. In simple words, this example represents a simple process of interrupting and restoring the biological clock. We can take a closer look at another similar example that can affect circadian rhythm which is the jetlag [1]. When people are traveling to a different country, in most cases, they suffer from jetlag. In other words, although people are in a different place, their internal circadian (biological) clock is still synchronized with their departure location. This inconsistency is the cause of people's inability to fall asleep during their first night of arrival. For these two examples, the entrainment to light-dark cycles enable the circadian system to align biological functions with appropriate times of day or night [2]. Many factors can affect the entrainment process, including light. In circadian biology, the phase response curve is commonly used to describe the synchronizing effects of light on a circadian pacemaker [3]. To create a phase response curve, discrete light stimuli are applied over the entire circadian cycle, and the magnitudes of light-induced phase shifts are plotted as a function of the circadian phase at which the cell/organism is exposed to the stimuli [3]. The major function of the phase response curve is to estimate the difference which denotes the phase shift between the initial circadian phase before the light stimulus and the final circadian phase after the light stimulus [3]. For instance, the phase response curve assists in showing the principle that delays are self-enhancing [4]. However, there are limitations to the phase response curve. The phase response curve might not accurately describe entrainment to photoperiods with substantial amounts of both light and dark given their reliance on a single limit cycle attractor [2]. The authors of [2] claim that they develop a 1-dimensional map that will produce a better prediction for phase-locking than methods than the phase response curve [2]. As written above, this 1-dimensional map is a relatively new method, which has not been widely applied in the research in the realm of the circadian rhythm. In addition, although the authors present the construction of this entrainment map for three circadian models in different dimensions, some details of constructing the entrainment map of a circadian model are still not included in [2]. The primary purpose of this paper is to investigate the possibility of constructing the entrainment for two additional models, which are the Becker-Weimann model and the Relogio model. The discussion of the challenges of constructing the entrainment map for a general circadian model is also included.

2 Models and Method

To begin with, we replicate the process of constructing the entrainment map for the Novak-Tyson model presented in [2]. Then, we will introduce the process of constructing the entrainment map for the Becker-Weimann model and the Relogio model.

2.1 Novak-Tyson Model

The Novak-Tyson model, presented in [2], is

$$\begin{aligned} \frac{1}{\phi}\cdot\frac{dP}{dt} &= M-(k_D+k_L\cdot f(t))\cdot P-k_f\cdot\frac{P}{0.1+P+2\cdot P^2}) \\ \frac{1}{\phi}\cdot\frac{dM}{dt} &= \epsilon\cdot(\frac{1}{1+P^4}-M) \end{aligned}$$

where all parameters are positive. The Novak-Tyson model for the molecular circadian clock in the fruit fly *Drosophila* includes 2 state variables in which M represents for mRNA concentration, and P represents for protein concentration [5]. Looking at $\frac{dP}{dt}$, one can realize that there exists an inhibitor term of P itself which results in a negative feedback loop. The parameter of ϵ is designed to have extremely small values leading to a separation

of time scales between variables P and M. The parameter ϕ determines the flow of trajectories in the phase plane. Parameter k_f denotes the scaling of the positive feedback because of the stabilization of the protein after dimerization. Parameter k_D indicates the default or the basic degradation rate of protein during darkness (without light). Similarly, parameter k_L indicates the added degradation rate of protein given the light input, usually referring to sunlight. $f(t)$ is a function that will determine whether there exists any light input or not. Range of $f(t)$ only contains two values: 1 and 0. When $f(t) = 0$, parameter k_L would be negated so that k_D exists in the model indicating it is situated in a completely dark environment; when $f(t) = 1$, the coefficient of the first inhibitor term, $k_D + k_L \cdot f(t)$, would become $k_D + k_L$ which indicates it is situated in an environment with light input. Notice that $f(t)$ is not a discontinuous step-wise function, it is designed as a smooth function that only takes values of 0 and 1. Following the fashion in [2], we use the following set of values for parameters in this model: $\phi = 2.1$, $k_D = 0.05$, $k_L = 0.05$, $k_f = 1$, and $\epsilon = 0.05$.

2.2 Becker-Weimann Model

The Becker-Weimann model is a 7-dimensional model for mammalian circadian oscillator designed for investigating the interdependence of the positive and negative feeback [6]. This model, defined in [6], is described by the following system of differential equations:

$$\frac{dy1}{dt} = \frac{v_{1b} \cdot (y7 + c)}{k_{1b} \cdot (1 + (\frac{y3}{k_{1i}})^p) + (y7 + c)} - k_{1d} \cdot y1. \tag{1}$$

$$\frac{dy2}{dt} = k_{2b} \cdot y1^q - k_{2d} \cdot y2 - k_{2t} \cdot y2 + k_{3t} \cdot y3 \tag{2}$$

$$\frac{dy3}{dt} = k_{2t} \cdot y2 - k_{3t} \cdot y3 - k_{3d} \cdot y3 \tag{3}$$

$$\frac{dy4}{dt} = \frac{v_{4b} \cdot y3^r}{k_{4b}^r + y3^r} - k_{4d} \cdot y4 \tag{4}$$

$$\frac{dy5}{dt} = k_{5b} \cdot y4 - k_{5d} \cdot y5 - k_{5t} \cdot y5 + k_{6t} \cdot y6 \tag{5}$$

$$\frac{dy6}{dt} = k_{5t} \cdot y5 - k_{6t} \cdot y6 + k_{7a} \cdot y7 - k_{6a} \cdot y6 \tag{6}$$

$$\frac{dy7}{dt} = k_{6a} \cdot y6 - k_{7a} \cdot y7 - k_{7d} \cdot y7. \tag{7}$$

Variable $y1$ represents the concentration of *Per2* or *Cry* mRNA. Variables $y2$ and $y3$ denote the concentrations of the *PER2/CRY* complex in the cytoplasm and the *PER2/CRY* complex in the nucleus respectively. Variable $y4$ represents the concentration of *Bmall* mRNA. Variable $y5$ of cytoplasmatic BMAL1 protein. Variable $y6$ denotes the BMAL1 protein in the nucleus. Lastly, variable $y7$ describes the concentration of a transcriptionally active form BMAL1. Apart from the interactions between all seven variables, one can notice that in every differential equation of each variable, there exists a self-inhibitory term to limit the growth of each variable. This system of ordinary differential equations is summarized in the graph below [6]:

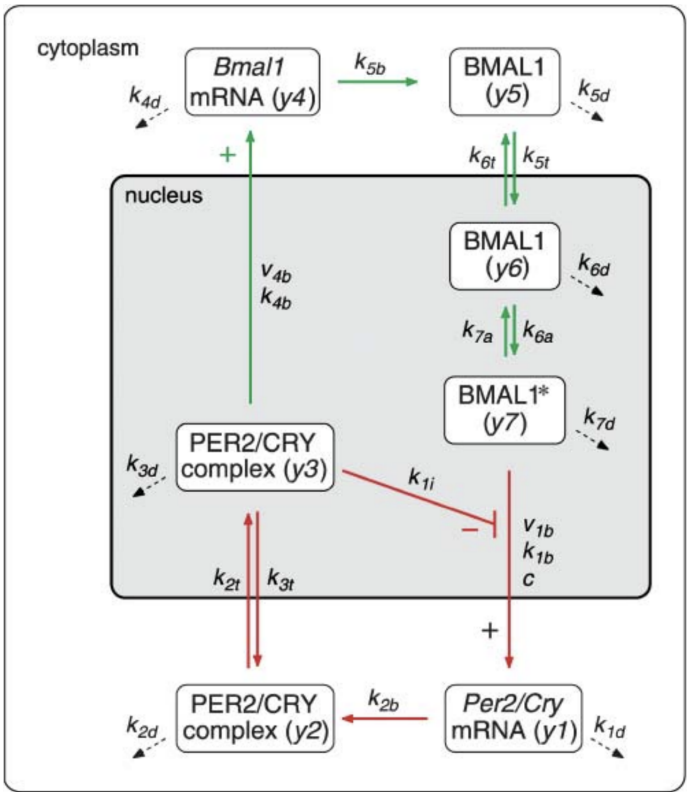

Figure 1. Graphic Representation of the System of Differential Equations of the Becker-Weimann model

The parameters that are chosen for this model are: $v_{1b} = 9$, $k_{1b} = 1$, $k_{li} = 0.56$, $c = 0.01$, $p = 8$, $k_{1d} = 0.12$, $k_{2d} = 0.05$, $q = 2$, $k_{2d} = 0.05$, $k_{2t} = 0.24$, k_{3t}, $k_{3t} = 0.02$, $k_{3d} = 0.12$, $v_{4b} = 3.6$, $k_{4b} = 2.16$, $r = 3$, $k_{4d} = 0.75$, $k_{5b} = 0.24$, $k_{5t} = 0.45$, $k_{6t} = 0.06$, $k_{6d} = 0.12$, $k_{6a} = 0.09$, $k_{7a} = 0.003$, and $k_{7d} = 0.09$. The light input is added to differential equation of $y1$ discretly, so that the differential equation of $y1$ becomes

$$\frac{dy1}{dt} = \frac{v_{1b} \cdot (y7 + c)}{k_{1b} \cdot (1 + (\frac{y3}{k_{li}})^p) + (y7 + c)} - k_{1d} \cdot y1 + LightInput.$$

The light input ($LightInput$) is described as the gated function below

$$LightInput = Light \cdot gate0 + Light \cdot gate1 \cdot (\frac{y3}{max(y3)})^{10} + Light \cdot gate2 \cdot (\frac{\frac{y4}{2} + y5}{max(y4y5)})^6.$$

However, in this paper, both $gate1$ and $gate2$ are both set to zero, and $gate0$ is set to 1. Therefore, we will simply have the equality of $LightInput = Light$. In simple words, we add the light stimulus directly and discretly to the first differential equation in the system for this model.

2.3 Relogio Model

The Relogio model is a 18-dimensional model for the mammadian circadian clock, which similarly, as Becker-Weimann model, allows for the study of the two main feedback loops: ROR/$Bmal$/REV-ERB and PER/CRY loop. This model accounts for the available experimental facts of the mouse core clock [7]. The system of differential

equations is as below:

$$
\begin{aligned}
\frac{dx1}{dt} &= k \cdot f_{x1} \cdot x7 - k \cdot d_{x1} \cdot x1 - d_{x1} \cdot x1 \\
\frac{dx2}{dt} &= k \cdot i_{z4} \cdot z4 - k \cdot e_{x2} \cdot x2 - d_{x2} \cdot x2 \\
\frac{dx3}{dt} &= k \cdot i_{z5} \cdot z5 - k \cdot e_{x3} \cdot x3 - d_{x3} \cdot x3 \\
PC &= x2 + x3 \\
\frac{dx5}{dt} &= k \cdot i_{z6} \cdot z6 - d_{x5} \cdot x5 \\
\frac{dx6}{dt} &= k \cdot i_{z7} \cdot z7 - d_{x6} \cdot x6 \\
\frac{dy1}{dt} &= V_{1max} \cdot \frac{1 + a \cdot (\frac{x1}{k_{t1}}^b)}{1 + (\frac{PC}{k_{i1}})^c \cdot (\frac{x1}{k_{t1}})^b + (\frac{x1}{k_{t1}})^b} - d_{y1} \cdot y1 + LightInput \\
\frac{dy2}{dt} &= V_{2max} \cdot \frac{1 + d \cdot (\frac{x1}{k_{t2}})^e}{1 + (\frac{PC}{k_{t2}})^f \cdot (\frac{x1}{k_{t2}})^e + (\frac{x1}{k_{t2}})^e} \cdot \frac{1}{1 + (\frac{x5}{k_{i21}})^{f1}} - d_{y2} \cdot y2 \\
\frac{dy3}{dt} &= V_{3max} \cdot \frac{1 + g \cdot (\frac{x1}{k_{t3}})^v}{1 + (\frac{PC}{k_{t3}})^w \cdot (\frac{x1}{k_{t3}})^v + (\frac{x1}{k_{t3}})^v} - d_{y3} \cdot y3 \\
\frac{dy4}{dt} &= V_{4max} \cdot \frac{1 + h \cdot (\frac{x1}{k_{t4}})^p}{1 + (\frac{PC}{k_{t4}})^q \cdot (\frac{x1}{k_{t4}})^p + (\frac{x1}{k_{t4}})^p} - d_{y4} \cdot y4 \\
\frac{dy5}{dt} &= V_{5max} \cdot \frac{1 + i \cdot (\frac{x6}{k_{t5}})^n}{1 + (\frac{x5}{k_{t5}})^m + (\frac{x6}{k_{t5}})^n} - d_{y5} \cdot y5 \\
\frac{dz1}{dt} &= k_{p2} \cdot (y2 + y2_0) + k \cdot d_{z4} \cdot z4 + k \cdot d_{z5} \cdot z5 - k \cdot f_{z5} \cdot z1 \cdot z2 - k \cdot f_{z4} \cdot z1 \cdot z3 - d_{z1} \cdot z1 \\
\frac{dz2}{dt} &= k_{p1} \cdot (y1 + y1_0) + k \cdot d_{z5} \cdot z5 + k \cdot d_{phz3} \cdot z3 - k \cdot f_{z5} \cdot z2 \cdot z1 - kph_{z2} \cdot z2 - d_{z2} \cdot z2 \\
\frac{dz3}{dt} &= kph_{z2} \cdot z2 + k \cdot d_{z4} \cdot z4 - k \cdot d_{phz3} \cdot z3 - k \cdot f_{z4} \cdot z3 \cdot z1 - d_{z3} \cdot z3 \\
\frac{dz4}{dt} &= k \cdot f_{z4} \cdot z1 \cdot z3 + k \cdot e_{x2} \cdot x2 - k \cdot i_{z4} \cdot z4 - k \cdot d_{z4} \cdot z4 - d_{z4} \cdot z4 \\
\frac{dz5}{dt} &= k \cdot f_{z5} \cdot z1 \cdot z2 + k \cdot e_{x3} \cdot x3 - k \cdot i_{z5} \cdot z5 - k \cdot d_{z5} \cdot z5 - d_{z5} \cdot z5 \\
\frac{dz6}{dt} &= k_{p3} \cdot (y3 + y3_0) - k \cdot i_{z6} \cdot z6 - d_{z6} \cdot z6 \\
\frac{dz7}{dt} &= k_{p4} \cdot (y4 + y4_0) - k \cdot i_{z7} \cdot z7 - d_{z7} \cdot z7 \\
\frac{dz8}{dt} &= k_{p5} \cdot (y5 + y5_0) - k \cdot i_{z8} \cdot z8 - d_{z8} \cdot z8
\end{aligned}
$$

In summary, $x1$ represents $CLOCK/BMAL$, $x2$ represents PER_N/CRY_N, $x3$ represents PER^*_N/CRY_N, PC represents PER/CRY_{pool}, $x5$ represents REV/ERB_N, $x6$ represents ROR_N, $y1$ represents Per, $y2$ represents Cry, $y3$ represents $Rev - Erb$, $y4$ represents Ror, $y5$ represents $Bmal$, $z1$ represents CRY_C, $z2$ represents PER_C, $z3$ represents PER^*_C, $z4$ represents PER^*_C/CRY_C, $z5$ represents PER_C/CRY_C, $z6$ represents $REV - ERB_C$, $z7$ represents ROR_C, and $z8$ represents $BMAL_C$. The light input is added discretly to the differential equation of Per ($y1$). The detailed interaction is described by the graph in [7] below

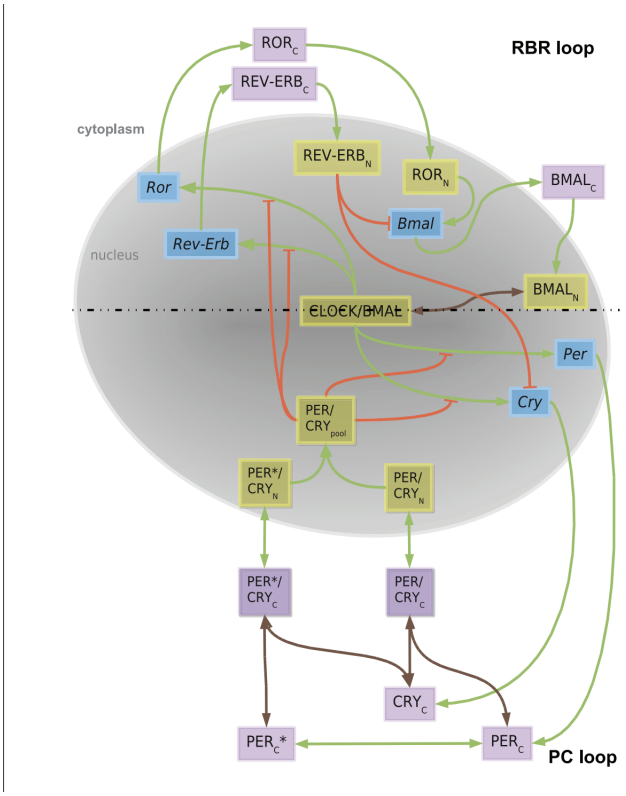

Figure 2. Graphic Representation of the System of Differential Equations of the Relogio Model

We used the following values for parameters: $d_{x1} = 0.08$, $d_{x2} = 0.06$, $d_{x3} = 0.09$, $d_{x5} = 0.17$, $d_{x6} = 0.12$, $d_{x7} = 0.15$, $d_{y1} = 0.3$, $d_{y2} = 0.2$, $d_{y3} = 2$, $d_{y4} = 0.2$, $d_{y5} = 1.6$, $d_{z1} = 0.23$, $d_{z2} = 0.25$, $d_{z3} = 0.6$, $d_{z4} = 0.2$, $d_{z5} = 0.2$, $d_{z6} = 0.31$, $d_{z7} = 0.3$, $d_{z8} = 0.73$, $k \cdot f_{x1} = 2.3$, $k \cdot d_{x1} = 0.01$, $k \cdot f_{z4} = 1$, $k \cdot d_{z4} = 1$, $k \cdot f_{z5} = 1$, $k \cdot d_{z5} = 1$, $kph_{z2} = 2$, $kd_{phz3} = 0.05$, $V_{1max} = 1$, $V_{2max} = 2.92$, $V_{3max} = 1.9$, $V_{4max} = 10.9$, $V_{5max} = 1$, $k_{t1} = 3$, $k_{i1} = 0.9$, $k_{t2} = 2.4$, $k_{i2} = 0.7$, $k_{i21} = 5.2$, $k_{t3} = 2.07$, $k_{i3} = 3.3$, $k_{t4} = 0.9$, $k_{i4} = 0.4$, $k_{t5} = 8.35$, $k_{i5} = 1.94$, $a = 12$, $d = 12$, $g = 5$, $h = 5$, $i = 12$, $k_{p1} = 0.4$, $k_{p2} = 0.26$, $k_{p3} = 0.37$, $k_{p4} = 0.76$, $k_{p5} = 1.21$, $k \cdot i_{z4} = 0.2$, $k \cdot i_{z5} = 0.1$, $k \cdot i_{z6} = 0.5$, $k \cdot i_{z7} = 0.1$, $k \cdot i_{z8} = 0.1$, $k \cdot e_{x2} = 0.02$, $k \cdot e_{x3} = 0.02$, $b = 5$, $c = 7$, $e = 6$, $f = 4$, $f1 = 1$, $v = 6$, $w = 2$, $p = 6$, $q = 3$, $n = 2$, $m = 5$, $y1_0 = 0$, $y2_0 = 0$, $y3_0 = 0$, $y4_0 = 0$, and $y5_0 = 0$.
The general process of constructing the entrainment map of a model can be summarized into two steps: (1) constructing the light-dark solution for 24 hours and (2) locating the *Poincare* (P) section.

3 Result

3.1 Replicating Entrainment Map for the Novak-Tyson Model

We first replicate the process of constructing the entrainment map for the Novak-Tyson model. Using the *scipy.integrate* package, we can first solve the system of differential equations with an initial condition of 0.1 for every variable from $t = 0$ to $t = 12$ for 12 hours without any light input (12 hours of a dark cycle), then continuing with the last point from the previous dark cycle, we will initiate another 12 hours cycle by solving the system of differential again using the endpoint from the last cycle as the initial condition with appropriate light input (12 hours of light cycle) from $t = 12$ to $t = 24$. In this way, a light-dark entrained solution (also named *LD Solution*) for the Novak-Tyson model is generated. Given that the Novak-Tyson model is consists of a 2-dimensional system of differential equations, we can plot the LD solution as the 2-dimensional space of variable M and P:

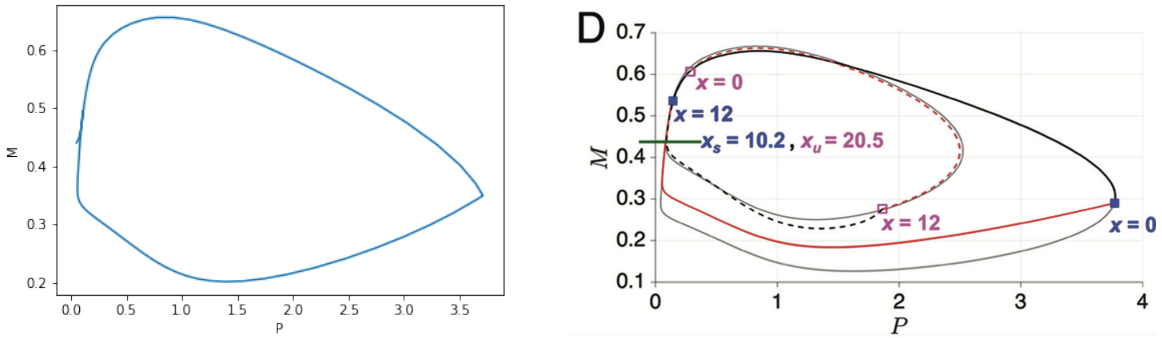

Figure 3. LD solution plotted using Python (left). Plot of the LD solution (solid black and solid red) presented in [2] (right).

We generate the same LD solution of the Novak-Tyson model like in [2] by the figure above. The next critical step is to choose the appropriate *Poincare* section. First, the *entrainment map* defined in [2] is a function that uses the potential effect of 12 hours light period and 12 hours dark cycle on the cycle duration as the response variable and time as an explanatory variable. By defining the entrainment map as $\Pi(x)$, this one-dimensional entrainment map would have the form as below

$$x_{n+1} = \Pi(x_n),$$

in which x_n denotes the number of hours from the moment that the lights turn on ($x = 0$) until the moment that the oscillator arrives at a certain location in the phase plane in the nth light-dark cycle. Since x can only take values of $[0, 24]$, given there are 24 hours in total in a single day, both the domain and range of the function of entrainment map $\Pi(x)$ is $[0, 24]$. Moreover, $\Pi(x)$ is a circle map with $x = 0$ same as $x = 24$ (the morning 0 am is the same as the evening 12 pm). For a n-dimensioanl circadian model, the Poincare section, denoted by P, is a $(n-1)$-dimensional hyperplane that intersects with the LD solution at a point. Since the hyperplane only intersects with the solution at one point, we only need to define the value of one of the variables and the direction of dynamics around the value. By specifying the direction of dynamics, it is equivalent to defining the sign of the first derivative around that point. Following the process in [2], P is defined at $M = 0.44$, with the direction of dynamics as $\frac{dM}{dt} > 0$. The codes that create the entrainment map are adapted from pseudocodes in the appendix of [2]. For the initial condition of the scipy function *integrate.solve_ivp*, we simply use the last point of the 24 hours LD entrained solution. To maximize the smoothness of the curve, instead of only integers from 0 to 24, we expand the set of inputs to all numbers from 0 to 24 with a 0.1 difference between two consecutive integers. The graphical representation of the Novak-Tyson model's entrainment map is

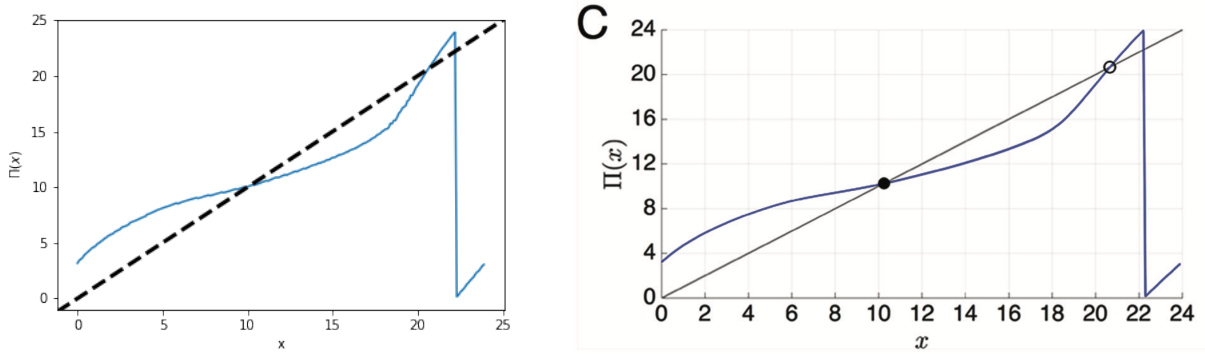

Figure 4. Novak-Tyson model's entrainment map plotted using Python (left). Plot of the Novak-Tyson model's entrainment map presented in [2] (right).

We generate the same graphical presentation of the entrainment map of the Novak-Tyson model as it in [2] by the figure above. The black dashed line represents the identity function which serves as a reference to the entrainment

map same as the solid black line in the plot of [2]. There exist two intersections between the entrainment map and the identity function, which are considered as two fixed points: one as the stable fixed point, the other one as the unstable fixed point [2]. By the definition, since the derivative of the entrainment map is less than zero ($|\Pi'(x_i)| < 1$) at the intersection at $x = 10.2$, the intersection at $x = 10.2$ is defined as a stable fixed point. For the other intersection at $x = 20.5$, since $\Pi'(x_i) > 1$ at this intersection, the intersection point at $x = 20.5$ is defined as an unstable fixed point. The stable fixed point corresponds to the stable LD-entrained solution, which means it will begin with experiencing $12 - 10.2 = 1.8$ hours of light before the LD-entrained solution started on P. Similarly, the unstable fixed point corresponds to the unstable LD-entrained solution, which denotes that it will start with experiencing $24 - 20.5 = 3.5$ hours of darkness before the LD-entrained solution started on P.

3.2 Generating Entrainment Map for Higher Dimensional Model

Based on the pseudocodes for generating the entrainment maps, there are three critical components of constructing an entrainment map: (1) the Poincare (P) section, (2) light input, and (3) the initial condition of the system of differential equations. In this section, we will discuss how would different choices of these three components affect the entrainment map. At the end of this section, we would present the 'best' entrainment maps for the Becker-Weimann and Relogio model that we could produce ('best' maps are defined as the maps that fit the standards of entrainment maps in [2] the most).

3.2.1 The Poincare Section

The authors of [2] define the Poincare section that is closely related to the initial conditions, in which the entrainment map should start with the initial condition that lies at the intersection of the Poincare section. Apart from this definition, there doesn't exist any specific instructions or requirement for picking the Poincare section. The first approach to locating the Poincare section that we used is using the nested loop to find the Poincare section. In detail, we wrap the pseudocodes of constructing the entrainment map in [2] inside of a nested loop. We only apply this approach to the Becker-Weimann model. Since the Poincare section is previously defined as a hyperplane, which is one dimension lower than the model, intersecting with the LD-entrained solution, to identify the crossing of the Poincare section, we only need to specify a single value of a particular variable such that if the solution curve of this particular variable crosses that value, then we can conclude that the trajectory reaches the Poincare section at certain times. In summary, the Poincare section is determined by specifying which variable is used, which point on the solution curve for this variable is used, and what the dynamic is around that point. There is only a finite number of variables in each of these higher dimensional models. There exists only two types of dynamics around a certain point ($\frac{d}{dt} \leq 0$ and $\frac{d}{dt} \geq 0$). In addition, the function for solving the initial value problem from the *scipy* package would output a finite number of solutions for a finite time interval. We also know the fact that the initial condition of the LD-entrained solution lies at the intersection of the Poincare section. There are only a finite number of choices of parameters for a given light input. Therefore, we first through every variable in the model, then loop through every value in the solution for each variable. For each round of the nested loop, the chosen value will be considered as the Poincare section and the initial condition (the values for the rest of the variables are picked using the same index of the chosen value in its respective variable), and the graphical presentation of the entrainment map would be generated for this chosen value. Due to the big scope of parameters for this search, we limit the domain of the entrainment map to be all integers from 0 to 24 (ends included) to exchange for greater computational efficiency. The trade-off is the smoothness of the curve. However, since the fundamental goal is to search for the optimal parameter for the Poincare section, the less smooth entrainment map curve is acceptable. Throughout the process of the nested loop, the dynamic around the intersection point between the Poincare section and the LD-entrained solution is assumed to be consistent. It is said that we set the dynamic around the intersection point to be positive ($\frac{d}{dt} \geq 0$) for one complete a nested loop and reset the dynamic around the intersection point to negative ($\frac{d}{dt} \leq 0$) for another complete nested loop. There are three typical types of graphical representation of the entrainment map generated from a complete nested loop regardless of the direction of the dynamic: (1) empty plot, (2) 'z'-shape curve, and (3) very rugged and oscillating curve, shown in Figure 5.

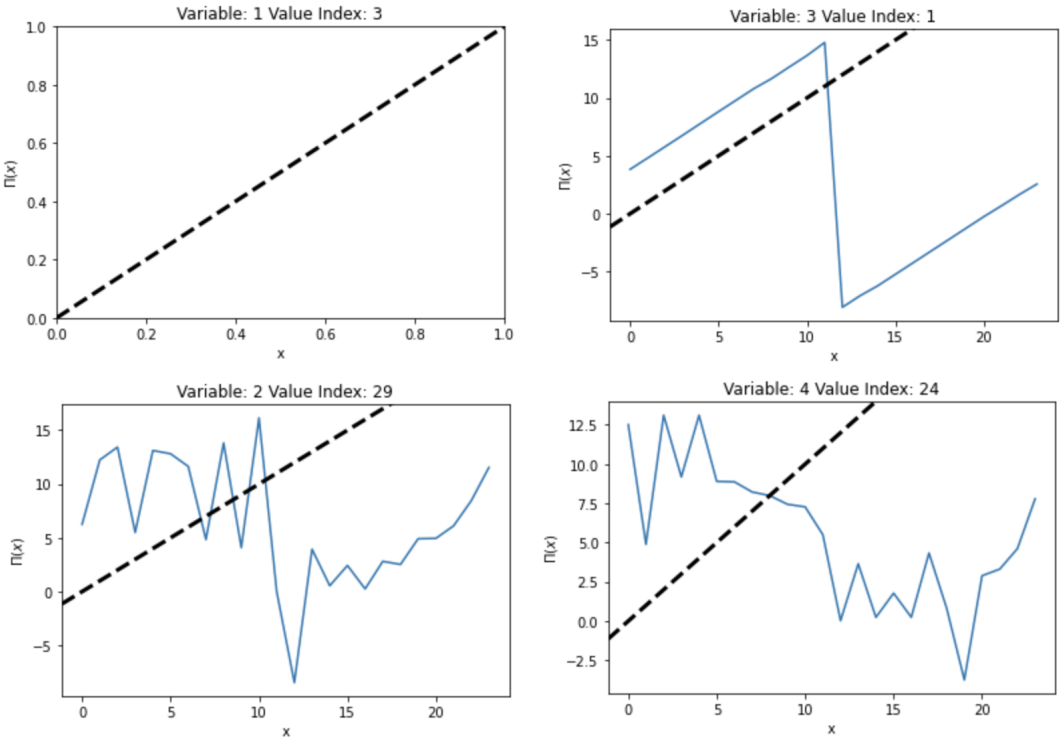

Figure 5. An example of empty plot of the entrainment map generated by the nested loop for the Becker-Weimann model (top left plot). An example of 'z'-shape curve of the entrainment map generated by the nested loop for the Becker-Weimann model (top right plot). Examples of the rugged and oscillating curve of the entrainment map generated by the nested loop for the Becker-Weimann model (bottom plots). All plots above are assuming that the dynamic around the Poincare section is positive.

The general reason for the empty plot is the bad choices in the Poincare section. With the difference in the numbers of explanatory and response variables, nothing can be plotted to the figure, resulting in an empty plot except for the identity function. In other words, for some of the inputs time, the algorithm is unable to estimate the time for the trajectory to reach the Poincare section, which also indicates the chosen Poincare section might be extremely off from the limit cycle for the LD-entrained solution so that the trajectory might be unable to even reach the Poincare section again once left. For the 'z'-shape curve of the entrainment map, it seems like there doesn't exist a dominant reason for that. We presume that it is also due to at least one bad choice of one of the critical parameters, including the Poincare section, light input, and initial condition. The reason for this 'z'-shape curve will be revisited later. The reason for the rugged and oscillating curves is very similar to that of the 'z'-shape curves, which is a bad choice of parameter sets. This method of searching using a nested loop fails almost entirely. The dominant issue is that none of the graphical representations of the entrainment map follows the definition or the standards of the entrainment map. Apart from the empty plot, many of the 'z'-shape curves have response variables with negative values which violate the range of the entrainment map function. All of the 'z'-shape curves would only cross with the identity function for exactly one time at $x = 12$. In this way, the 'z'-shape curves would always denote the existence of a stable fixed point ($\frac{d}{dt} < 0$ at $x = 12$) that corresponds to the stable LD-entrained solution. In other words, the 'z'-shape curves will not include any useful information regarding the properties of the entrained solution of every model. The rugged and oscillating curves are quite similar to the 'z'-shape curves except for one remark that it might cross the identity functions more than two times. The existence of multiple stable fixed points will also not include useful information regarding the properties of the entrained solution of every model. The result of the method of searching using the nested loop with the assumption of negative dynamic yields the same result as that with the assumption of positive dynamic.

3.2.2 Light Input

Different light input will affect the entrainment map tremendously. A very large amount of light input will result of the empty plots. With a very large amount amount input, the trajectory would never reach back to the Poincare section again leading to the problem of inconsistent number of values for explanatory and response variable. Apart from the empty plots, a very large amount of light input can lead to a curve that oscillates for a huge value but in very short interval of x, shown in Figure 6.

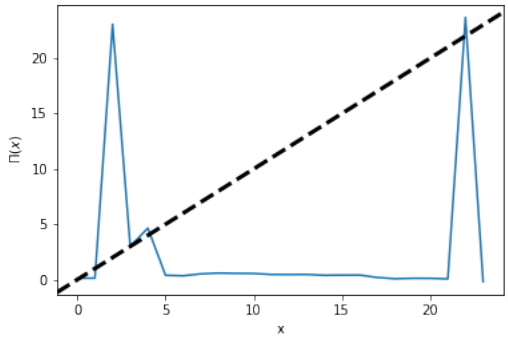

Figure 6. An example of the curve of the entrainment map with very large light input (1 for light input) for the Relogio model.

Shrinking the light input would make the curve for the entrainment map look similar to the rugged and oscillating curve defined earlier while controlling for all other parameters, shown in Figure 7.

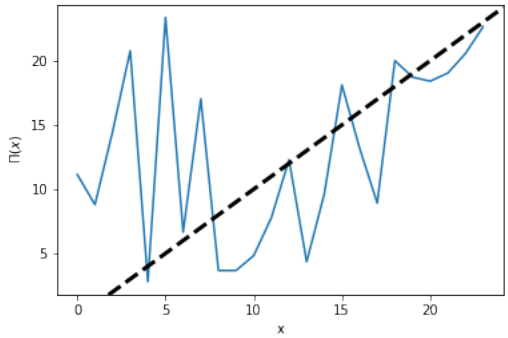

Figure 6. An example of the curve of the entrainment map with a smllaer light input (0.05 for light input) for the Relogio model.

In addition, it seems like an extremely small amount of light input would result a similar rugged and oscillating curve as the one in Figure 7.

3.2.3 Initial Condition

Only changing the initial condition alone will not have a large impact on the entrainment map in general. However, certain choices for the initial condition and the Poincare section under the assumption that the entrainment map starts with the initial condition that lies at the intersection of the Poincare section will generate 'z'-shape curves. Apart from that, only changing the initial condition will most likely cause the minor vertical shift of a rugged and oscillating curve or the change in the number of oscillations of a rugged and oscillating curve.

3.2.4 Delay of Entering the Limit Cycle

Even with the above understanding of the three important parameters of the entrainment map, we are still unable to generate an appropriate entrainment map for either the Becker-Weimann model or the Relogio model. Inspired by Professor Stephanie Taylor, we realize that problem is not only with the bad choices of parameters but also with the limit cycle itself. Referring back to the LD-entrained solution of the Novak-Tyson model generated by Python in Figure 3, one would notice that starting at $t = 0$, the trajectory is already in the limit cycle. In this way, the algorithm of constructing the entrainment map would function perfectly on the Novak-Tyson model beginning with $t = 0$. However, the situations for the Becker-Weimann model and the Relogio model are different from that of the Novak-Tyson model. Both of the higher dimensional models are not in their respective limit cycle at $t = 0$. The plots for each variable of the LD-entrained solution of each model from $t = 0$ to $t = 120$ confirms this idea, shown in Figure 7.

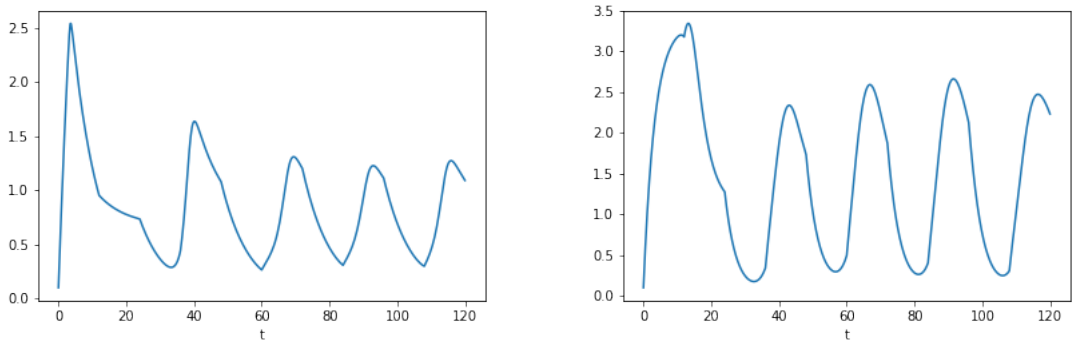

Figure 7. Plot for the first variable of the LD-entrained solution of the Becker-Weimann model from $t = 0$ to $t = 120$ (left). Plot for the eleventh variable of the LD-entrained solution of the Relogio model from $t = 0$ to $t = 120$ (right).

In this way, we let both models simulate for 120 hours first so that both of them can enter their respective limit cycles definitively. Then, on top of that, the algorithm for constructing the entrainment is performed. Moreover, we also loosen the requirement that the entrainment map must start with the initial condition that lies at the intersection of the Poincare section. We allow the initial condition to be in the close neighborhood of the Poincare section so that there is more freedom in choosing critical components.

3.2.5 Entrainment Maps for the Becker-Weimann Model and the Relogio Model

By letting both models to simulate for 120 hours first and carefully picking the critical components, we manage to generate the entrainment maps for both models with the best set of parameters that we can find.

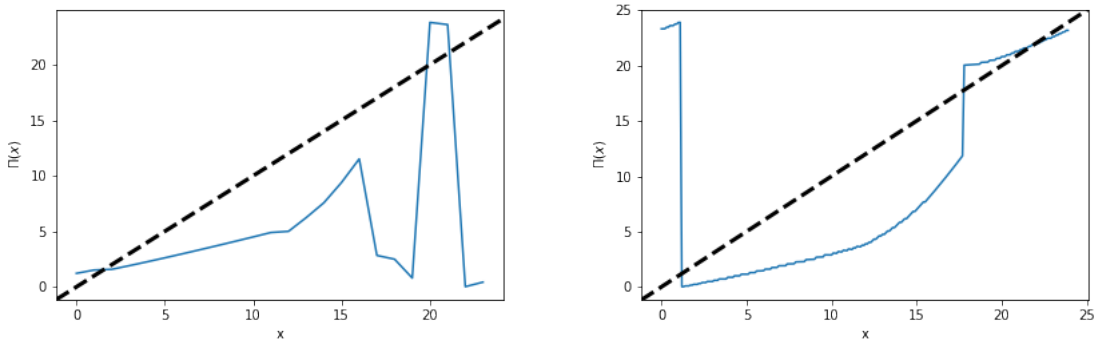

Figure 8. Entrainment map for the Becker-Weimann model (left) and the entrainment map for the Relogio model (right) generated with the best set of parameters that we can find.

For the Becker-Weimann model, we use the endpoint of the 120 hours simulation of the LD-entrained solution as the initial condition. The light input is set to be 0.08. The Poincare section is set to be 0.95 for the first variable in the system. The dynamic around the Poincare section is set to be positive. One unstable fixed point is located at $x = 19.5$. For the Relogio model, we still use the endpoint of the 120 hours simulation of the LD-entrained solution as the initial condition. The light input is set to be 0.32. The Poincare section is set to be 1.5 for the eleventh variable in the system. The dynamic around the Poincare section is set to be positive. One stable fixed point is located at $x = 18.1$. One unstable fixed point is located at $x = 21.9$.

4 Conclusion

There are still some problems with the entrainment map for either the Becker-Weimann model or the Relogio model. For the entrainment map for the Becker-Weimann model, one of the problems is that there doesn't exist a stable fixed point. In addition, the other problem is that the dynamic of the curve for the entrainment map shifts to negative of a sudden at around $x = 16$ and shift to positive in an extremely tiny time interval. For the entrainment map for the Relogio model, the drastic drop in $\Pi(x)$ should happen at around $x = 23$ instead if starts with a very high value for the response variable in the beginning at round $x = 0$. We, first, assume it is an issue due to the bad choice of the initial condition since an initial condition that deviates from the Poincare section too much would very likely lead to the curve starting with a value for the response variable that is far from the identity function. However, even after the initial condition is readjusted, the entrainment map does not better, instead, we obtain a rugged and oscillating curve for the entrainment map which is not desired. Fortunately, the authors of [2] have shown that the curve for the Relogio model presented in Figure 8 is a consequence of employing a different set of parameters for the model itself. In general, it is viable to construct an entrainment map for other circadian models. However, it is not an efficient approach since there doesn't exist a definitive set of steps for constructing it. The method developed in this paper will require careful examinations of the limit cycle of every variable in a model and many trials of the fitting. Moreover, there exist many critical parameters of the entrainment map, including initial condition, light input, and the Poincare section, and parameters of the model itself that are required to be chosen appropriately to construct the proper entrainment maps. The primary limitation of this paper is that we only use one set of parameters for each model. As discussed in [2], different choices of model parameters will lead to a horizontal shift of the curve for the entrainment map. Future work can concentrate on exploring the effect of employing a different set of parameters on the respective entrainment map.

References

[1] Circadian Rhythms. National Institute of General Medical Sciences. 2022. https://www.nigms.nih.gov/education/fact-sheets/Pages/circadian-rhythms.aspx

[2] Diekman, C. O., & Bose, A. (2016). Entrainment Maps: A New Tool for Understanding Properties of Circadian Oscillator Models. Journal of Biological Rhythms, 31(6), 598–616. https://doi.org/10.1177/0748730416662965

[3] Charles A. Czeisler, Orfeu M. Buxton, Chapter 35 - Human Circadian Timing System and Sleep-Wake Regulation, Editor(s): Meir Kryger, Thomas Roth, William C. Dement, Principles and Practice of Sleep Medicine (Sixth Edition), Elsevier, 2017, Pages 362-376.e5, ISBN 9780323242882, https://doi.org/10.1016/B978-0-323-24288-2.00035-0.(https://www.sciencedirect.com/science/article/pii/B9780323242882000350)

[4] Taylor SR (2021) Delays are Self-enhancing: An Explanation of the East-West Asymmetry in Recovery from Jetlag. J. Biol. Rhythms, 074873042199048.

[5] Novák, B., Tyson, J. Design principles of biochemical oscillators. Nat Rev Mol Cell Biol 9, 981–991 (2008). https://doi.org/10.1038/nrm2530

[6] Becker-Weimann S, Wolf J, Herzel H, Kramer A. Modeling feedback loops of the Mammalian circadian oscillator. Biophys J. 2004 Nov;87(5):3023-34. doi: 10.1529/biophysj.104.040824. Epub 2004 Sep 3. PMID: 15347590; PMCID: PMC1304775.

[7] Relógio A, Westermark PO, Wallach T, Schellenberg K, Kramer A, Herzel H. Tuning the mammalian circadian clock: robust synergy of two loops. PLoS Comput Biol. 2011 Dec;7(12):e1002309. doi: 10.1371/journal.pcbi.1002309. Epub 2011 Dec 15. PMID: 22194677; PMCID: PMC3240597.